Standard J. 12: 345–678 (2013)
DOI 10.1007/s00815-002-6789-z

GENERIC ARTICLE CATEGORY

Carine Moussaed · Stephen Wornom · Maria-Vittoria Salvetti · Bruno Koobus · Alain Dervieux

Impact of dynamic subgrid scale modeling in variational multiscale large-eddy simulation of bluff-body flows

Received:/ Accepted: / Published online:

Abstract The effects of dynamic subgrid scale (SGS) models are investigated in variational multiscale (VMS) LES simulations of bluff-body flows. The spatial discretization is based on a mixed finite element/finite volume formulation on unstructured grids. In the VMS approach used in this work, the separation between the largest and the smallest resolved scales is obtained through a variational projection operator and a finite volume cell agglomeration. The dynamic version of Smagorinsky and WALE SGS models are used to account for the effects of the unresolved scales. In the VMS approach, these effects are only modeled in the smallest resolved scales. The dynamic VMS-LES approach is applied to the simulation of the flow around a circular cylinder at Reynolds numbers 3900 and 20000 and to the flow around a square cylinder at Reynolds numbers 22000 and 175000. It is observed that the dynamic SGS procedure has a smaller impact on the results within the VMS approach than in LES. However, the global accuracy of the predictions is improved for dynamic SGS models with a small computational extra cost.

Keywords variational multiscale LES · dynamic SGS model · unstructured grids · circular cylinder · square cylinder.

1 Introduction

In spite of an extensive research for more than a century applied to the flows in turbulent regime, their modelling remains a big challenge even today. Direct Numerical Simulation (DNS), which numerically resolves all the significant scales of motion in a flow down to the Kolmogorov scales, is still not practical for engineering applications. Large Eddy Simulation (LES) directly computes the large-scale turbulent structures, which are responsible for the largest part of the transfer of energy and momentum in a flow, while modelling the smaller dissipative and more isotropic structures. Today LES is increasingly used in industrial applications, at least for those flows for which the statiscal approach, which consists in time-averaging the Navier-Stokes (RANS) equations, encounters difficulties in giving accurate predictions. Paradigmatic examples of such flows are bluff-body wakes. A RANS calculation is little dependent on the Reynolds number and little greedy in CPU time,

C. Moussaed · B. Koobus
I3M, Université Montpellier 2, Place Eugène Bataillon, 34095 Montpellier cedex, France
E-mail: carine.moussaed@univ-montp2.fr, koobus@math.univ-montp2.fr

S. Wornom
LEMMA, 2000 Route des Lucioles, 06902 Sophia-Antipolis, France
E-mail: Stephen.Wornom@inria.fr

M.V. Salvetti
Dipartimento di Ingegneria Aerospaziale,Università di Pisa, Via G. Caruso 8, 56122 Pisa, Italy
E-mail: mv.salvetti@dia.unipi.it

A. Dervieux
INRIA, 2004 Route des Lucioles, 06902 Sophia-Antipolis, France
E-mail: alain.dervieux@sophia.inria.fr

but provides only a limited information. Moreover, RANS modelling presents a strong degree of empiricism, making this approach scarcely reliable for various types of flow. LES is the midway between DNS and RANS modelling as for both the amount of information available from the simulations and the computational costs.

As a sequel of the pioneering work of Smagorinsky [1], an important class of LES models relies on the addition to the Navier-Stokes equations of an eddy-viscosity term applying some dissipation to the flow. The dissipation introduced on the resolved scales by the Smagorinsky model relies on second derivatives of the filtered velocity fields; it can be easily shown by a Fourier analysis that this yields a significant damping also of the largest resolved scales; for instance, the damping of a scale twice larger than another one is roughly only four times lower than that of the smaller scale. The definition of the weight of this term is also of delicate choice and paramount impact. It has been early seen that Smagorinsky first proposal was not adequate for boundary layers. Many methods have been proposed for overcoming the near-wall accuracy problem with some damping of the SGS coefficient or, with an adapted choice of the flow gradient evaluation as in the Wall-Adapted Local Eddy viscosity (WALE) model of [2]. However, the WALE model still suffers of some of the drawbacks of the Samgorinsky models, as for instance the fact that the constant present in the eddy-viscosity term is flow dependent, i.e. it needs to be tuned in order to enjoy the best accuracy for different types of flow.

Then it seems necessary to apply a particular procedure in order to "adjust the constant" as a *non spatially uniform and non time-constant* parameter in eddy-viscosity models. The dynamic method [5] addresses this issue and can be combined with many existing eddy-viscosity models. It has been observed that the dynamic method overcomes most of the drawbacks of the Smagorinsky model, viz. the incorrect behavior near solid walls and in laminar flows, the lack of backscatter of energy and the need of a-priori tuning the model constant.

However, the fact that the model parameter is allowed to vray in space and time does not automatically correspond to a discrimination of the damping effects of the eddy-viscosity term on the different scales. A variational multiscale (VMS) formulation of LES has been proposed in [3]. It is aimed at reducing the excessive dissipation introduced by eddy-viscosity SGS models also on the large scales. VMS-LES does it by decomposing, through Galerkin projection, the resolved scales into the largest and smallest ones and by adding the SGS model only to the smallest ones. It has been noted that using VMS-LES also solves the problem encountered by Smagorinsky-like models at boundary layers. But, again, this method has a larger spectrum of potentialities and, since its mechanism concerns a different dimension, it can make a complementary job to a dynamic formulation.

In this work, we investigate the effect of employing dynamic SGS models in the VMS-LES approach, used together with an industrial numerical set-up. This industrial numerical set-up, based on a mixed finite-volume/finite-element discretization, is performed on rather coarse unstructured grids as those often used in industrial applications. The VMS approach is particularly attractive for variational numerical methods and unstructured grids, because it is easily incorporated in such formulations [4] and the additional computational costs with respect to classical LES are very low. The used VMS approach is the one proposed in [4], in which the projection operator in the largest resolved scale space is defined through finite-volume cell agglomeration. Two different dynamic eddy-viscosity SGS models are considered viz. the dynamic version [5,6] of Smagorinsky [1] and WALE models.

Very few dynamic VMS-LES simulations have been performed in the past. A dynamic VMS-LES method was introduced in [7]. A coarse mesh made of macro-cells defined by an agglomeration process, was used in the variational form brought by the VMS method in order to determine the dynamic SGS model coefficient varying in space and time. This approach is different from the present one, in which the Germano algebraic identity is used independantly of the variational formulation. In [7], the test cases of a prolate spheroid and of a forward swept wing where considered. The authors conclude that the proposed dynamic VMS-LES procedure captures small turbulence structures that are not resolved by its static counterpart, but this does not improve significantly integral quantities such as lift and drag predicted by the static VMS-LES method.

In the more recent work of Gravemeier [8] a VMS-LES approach is combined with a dynamic Smagorinsky model in slightly different formulations for the simulation of a turbulent flow in a diffuser. According to this latter work, passing from VMS to dynamic-VMS did not brought a significant improvement.

In the present paper, we focus on VMS-LES simulations of bluff-body flows carried out with the above non-dynamic SGS models as well as with their dynamic counterpart, in order to evaluate the impact of the dynamic procedure on the SGS viscosity and on the simulation results. To this aim we consider the flow around a circular cylinder at Reynolds numbers 3900 and 20000, and the flow around a square cylinder at Reynolds numbers 22000 and 175000. Bluff bodies were already successfuly addressed in [9,10] for various Reynolds numbers with VMS-LES and the aim of the present work is to investigated whether further improvements can be obtained with dynamic models.

2 Variational Multiscale LES approach

The VMS formulation consists in splitting between the large resolved scales (LRS) i.e. those resolved on a virtual coarser grid, and the small resolved ones (SRS) which correspond to the finest level of discretization. The VMS-LES method does not compute the SGS component of the solution, but it models its dissipative effects on the SRS, and it preserves the Navier-Stokes model for the large resolved scales.

2.1 VMS formulation

In the present work, we adopt the VMS approach proposed in [4] for the simulation of compressible turbulent flows through a finite volume/finite element discretization on unstructured tetrahedral grids. Let V_{FV} be the space spanned by ψ_k, the finite volume basis function, and V_{FE} the one spanned by ϕ_k, the finite element basis function. In order to separate large and small scales, these spaces are decomposed as: $\psi_k =< \psi_k > +\psi'_k$ and $\phi_k =< \phi_k > +\phi'_k$ where the *brackets* denote a coarse scale and the *prime* a fine scale. Consequently to this decomposition, the variables of the flow are decomposed as follows:

$$W =< W > +W' + W^{SGS} \tag{1}$$

where $< W >$ are the LRS, W' the SRS and W^{SGS} are the unresolved scales. In [4] , a projector operator based on spatial average on macro-cells is defined to determine the basis functions of the LRS space:

$$< \psi_k >= \frac{Vol(C_k)}{\sum_{j\epsilon I_k} Vol(C_j)} \sum_{j\epsilon I_k} \psi_j \quad ; \quad \psi'_k = \psi_k - < \psi_k > \tag{2}$$

for finite volumes, and

$$< \phi_k >= \frac{Vol(C_k)}{\sum_{j\epsilon I_k} Vol(C_j)} \sum_{j\epsilon I_k} \phi_j \quad ; \quad \phi'_k = \phi_k - < \phi_k > \tag{3}$$

for finite elements. $Vol(C_j)$ denotes the volume of C_j, the cell around the vertex j, and $I_k = \{ j/C_j \in C_{m(k)} \}$ where $C_{m(k)}$ is the macro-cell containing the cell C_k. The macro-cells are obtained by a process known as agglomeration [11]. The SGS model which introduces the dissipative effect of the unresolved scales on the resolved scales is only added to the SRS. Let $\Phi = (\phi^1, \phi^2, \phi^3, \phi^4, \phi^5)$ the test functions for the Navier-Stokes system. Superscripts hold for the components entering in each equation of the system. We use the notation $\Phi_{234} = (\phi^2, \phi^3, \phi^4)$. The term below is added to the momentum equations

$$\begin{aligned} &\int_\Omega \tau' \cdot \nabla \Phi'_{234} \, d\Omega \qquad \text{with} \\ \tau'_{ij} &= -\mu'_{sgs}(2S'_{ij} - \frac{2}{3} S'_{kk}\delta_{ij}) \\ S'_{ij} &= \frac{1}{2}(\frac{\partial u'_i}{\partial x_j} + \frac{\partial u'_j}{\partial x_i}) \end{aligned} \tag{4}$$

where μ'_{sgs} denotes the viscosity of the SGS model used to close the problem, computed as a function of the smallest resolved scales. Likewise, the term

$$\int_\Omega \frac{C_p \mu'_{sgs}}{Pr_{sgs}} \nabla T' \cdot \nabla \Phi'_5 \, d\Omega \tag{5}$$

is added to the energy equation. C_p is the specific heat at constant pressure and Pr_{sgs} is the subgrid-scale Prandtl number which is assumed to be constant.

2.2 SGS viscosities

The SGS terms appearing in the LES equations must be expressed through a SGS model. The most commonly used SGS model in LES is the Smagorinsky model [1] in which the eddy viscosity is defined by

$$\mu_{\text{sgs}} = \overline{\rho}\,(C_{\text{s}}\Delta)^2 \left|\widetilde{S}\right| \quad , \tag{6}$$

where Δ is the filter width, C_{s} is the Smagorinsky coefficient and $\left|\widetilde{S}\right| = \sqrt{2\widetilde{S_{ij}}}$. The *overline* denotes the grid filter and the *tilde* holds for Favre averaging, $\tilde{f} = \overline{\rho f}/\overline{\rho}$. The filter width is defined as the third root of the grid element volume. A typical value for the Smagorinsky coefficient is $C_s = 0.1$ which is used, especially for shear flows.

The second SGS model we considered is the Wall-Adapting Local Eddy -Viscosity (WALE) SGS model proposed by Nicoud and Ducros [2]. The eddy-viscosity term μ_{sgs} is then defined by:

$$\mu_{\text{sgs}} = \overline{\rho}(C_W\Delta)^2 \frac{(\widetilde{S_{ij}}^d \widetilde{S_{ij}}^d)^{\frac{3}{2}}}{(\widetilde{S_{ij}}\widetilde{S_{ij}})^{\frac{5}{2}} + (\widetilde{S_{ij}}^d \widetilde{S_{ij}}^d)^{\frac{5}{4}}} \tag{7}$$

with $\widetilde{S_{ij}}^d = \frac{1}{2}({g_{ij}}^2 + {g_{ji}}^2) - \frac{1}{3}\delta_{ij}{g_{kk}}^2$ being the symmetric part of the tensor ${g_{ij}}^2 = g_{ik}g_{kj}$, where $g_{ij} = \partial\tilde{u}_i/\partial x_j$. As indicated in [2], the constant C_W is set to 0.5.

In the case of a combination of VMS-LES with either of these two eddy viscosity models, $\widetilde{S_{ij}}$ and $\widetilde{S_{ij}}^d$ need to be replaced by S'_{ij} and $(S^d_{ij})'$respectively.

2.3 Dynamic model

In their original formulations, the constant (C_s, C_w) appearing in the expression of the viscosity of the Smagorinsky and WALE SGS model (Eqs. (6) and (7) respectively) were set to a constant over the entire flow field. For general inhomogeneous flows, however, the SGS viscosity can significantly vary in space. In the dynamic procedure, this constant is then replaced, according to Germano *et al.* [5], by a dimensionless parameter $C(x,t)$ that is allowed to be a function of space and time. The dynamic approach provides a systematic way for adjusting the model constant in space and time, which is desirable for complex turbulent flows. An interesting and appealing feature of this method is that $C(x,t)$ is dynamically estimated using information from the resolved scales making the model self-tuning. The so-called dynamic model [5] has been successfully used to study a variety of complex inhomogeneous flows. After the introduction of the grid filter, denoted by *overline* and *tilde*, a second step in the dynamic model consists in the introduction of a second filter, having a larger width than the grid one, which is called the test-filter and denoted by a *hat*. The test-filter is applied to the grid filtered Navier Stokes equations, and then, the subtest-scale stress is defined as follows:

$$M_{ij}^{test} = \widehat{\overline{\rho}\overline{\mathbf{u}_i}\overline{\mathbf{u}_j}} - \left(\hat{\overline{\rho}}\right)^{-1}\left(\widehat{\overline{\rho}\overline{\mathbf{u}_i}}\,\widehat{\overline{\rho}\overline{\mathbf{u}_i}}\right) \tag{8}$$

The deviatoric part of M_{ij}^{test} can be written using a Smagorinsky or WALE model, as

$$M_{ij}^{test} - \frac{1}{3}M_{kk}^{test}\delta_{ij} \;=\; -C\hat{\Delta}^2\hat{\overline{\rho}}g(\hat{\tilde{\mathbf{u}}})\hat{\tilde{P}}_{ij} \quad (C \;=\; {C_w}^2 \text{ or } {C_s}^2) \tag{9}$$

with $\hat{\tilde{P}}_{ij} = -\frac{2}{3}\hat{\tilde{S}}_{kk}\delta_{ij} + 2\hat{\tilde{S}}_{ij}$ and where $g(\hat{\tilde{\mathbf{u}}})$ denotes the contribution to the SGS viscosity depending on the gradient velocity that appears in (6) for the Smagorinsky model, and in (7) for the WALE model. The constant C, as originally proposed by Germano *et al.* [5], is assumed to be constant at the subgrid and subtest levels.

Let us now introduce the quantity

$$\mathcal{L}_{ij} = M_{ij}^{test} - \hat{M}_{ij} = \widehat{\overline{\rho}\tilde{\mathbf{u}}_i\tilde{\mathbf{u}}_j} - \left(\hat{\overline{\rho}}\right)^{-1}\left(\widehat{\overline{\rho}\tilde{\mathbf{u}}_i}\widehat{\overline{\rho}\tilde{\mathbf{u}}_i}\right) \tag{10}$$

called the Leonard stress, which is known from a LES computation. In order to determine the constant C, one can relate $\mathcal{L}_{ij}$ to the value obtained using the SGS model (Smagorinsky or WALE). This leads to

$$L_{ij} = \mathcal{L}_{ij} - \frac{1}{3}\mathcal{L}_{kk}\delta_{ij} \;=\; (C\Delta^2)B_{ij} \tag{11}$$

where

$$B_{ij} \;=\; \widehat{\bar{\rho}g(\tilde{\mathbf{u}})\tilde{\bar{P}}_{ij}} - \left(\frac{\hat{\Delta}}{\Delta}\right)^2 \hat{\bar{\rho}}g(\hat{\tilde{\mathbf{u}}})\hat{\tilde{\bar{P}}}_{ij}.$$

Equation (11) is a tensorial relationship in one unknown $(C\Delta^2)$ which has to satisfy:

$$L_{ij} = (C\Delta^2)B_{ij}. \tag{12}$$

This system of six equations can be contracted using the least squares approach [6]. Therefore, $(C\Delta^2)$ should minimize the quantity

$$Q = (L_{ij} - (C\Delta^2)B_{ij})^2. \tag{13}$$

Thus, $(C\Delta^2)$ is found by setting $\frac{\partial Q}{\partial (C\Delta^2)} = 0$; this gives $(C\Delta^2)$:

$$(C\Delta^2) = \frac{L_{ij}B_{ij}}{B_{pq}B_{pq}}\ . \tag{14}$$

A possible drawback of the dynamic procedure based on the Germano-identity [5] when applied to a SGS model already having a correct near-wall behavior, as the WALE one, is the introduction of a sensitivity to the additional filtering procedure. A simple way to avoid this inconvenient is to have a sensor able to detect the presence of the wall, without a priori knowledge of the geometry, so that the dynamic SGS model adapts to the classical constant of the model, which is equal to 0.5 in the near wall region for the WALE model, and compute the constant dynamically otherwise. We adopt the sensor proposed in [12], having the following expression:

$$SVS = \frac{(\widetilde{S_{ij}}^d \widetilde{S_{ij}}^d)^{\frac{3}{2}}}{(\widetilde{S_{ij}}^d \widetilde{S_{ij}}^d)^{\frac{3}{2}} + (\widetilde{S_{ij}}\widetilde{S_{ij}})^3}. \tag{15}$$

This parameter has the properties to behave like y^{+3} near a solid wall, to be equal to 0 for pure shear flows and to 1 for pure rotating flows.

It should be noticed that the implementation of the dynamic SGS models in our software has been optimized so that the additional cost of the resulting dynamic LES and VMS models, in the case of an implicit time-marching scheme, which is our default option, is less than 1% compared to their non-dynamic counterparts.

3 Numerical discretization

We briefly recall now the main features of the numerical scheme. Further details can be found in [13] and in [14].

The governing equations are discretized in space using a mixed finite volume/finite element method applied to unstructured tetrahedrizations. The adopted scheme is vertex centered, i.e. all degrees of freedom are located at the vertices. P1 Galerkin finite elements are used to discretize the diffusive terms.

A dual finite-volume grid is obtained by building a cell C_i around each vertex i; the finite-volume cells are built by the rule of medians: the boundaries between cells are made of triangular interface facets. Each of these facets has a mid-edge, a facet centroid, and a tetrahedron centroid as vertices. The convective fluxes are discretized on this tessellation by a finite-volume approach, i.e. in terms of the fluxes through the common boundaries between each couple of neighboring cells. The unknowns are discontinuous along the cell boundaries and this allows an approximate Riemann solver to be introduced. The Roe scheme [15] (with low-Mach preconditioning) represents the basic upwind component for the numerical evaluation of the convective fluxes. The MUSCL linear reconstruction method ("Monotone Upwind Schemes for Conservation Laws"), introduced by Van Leer [16], is adapted for increasing the spatial accuracy. The basic idea is to express the Roe flux as a function of reconstructed values of W at the boundary between two neighboring cells. Attention

has been dedicated to the dissipative properties of the resulting scheme which is a key point for its successful application to LES simulations.The numerical dissipation in the resulting scheme is made of sixth-order space derivatives by using suited reconstructions [13]. Time advancing is carried out through an implicit linearized method, based on a second-order accurate backward difference scheme and on a first-order approximation of the Jacobian matrix [17]. The resulting numerical discretization is second-order accurate both in time and space.

4 Applications

4.1 Circular cylinder test-case, Reynolds number 20000

Simulations for the flow around a circular cylinder are carried out at Reynolds number based on the cylinder diameter, D, and the freestream velocity, equal to 20000. The computational domain is such that $-10 \leq x/D \leq 25$, $-20 \leq y/D \leq 20$ and $-\pi/2 \leq z/D \leq \pi/2$, where x, y and z denote the streamwise, transverse and spanwise directions respectively, the cylinder axis being located at $x = y = 0$. Periodic boundary conditions are applied in the spanwise direction while no-slip conditions are imposed on the cylinder surface. Characteristic based conditions are used at the inflow and outflow as well as on the lateral surfaces. The freestream Mach number is set equal to 0.1 in order to make a sensible comparison with incompressible simulations in the literature. Preconditioning is used to deal with the low Mach number regime. The computational domain is discretized by an unstructured grid consisting of approximately 1.8 million of nodes. The averaged distance of the nearest point to the cylinder boundary is 0.001D, and 100 nodes are present in the spanwise direction near the cylinder, with an approximately uniform distribution. LES and VMS-LES simulations have been carried on this grid for the WALE and the Smagorinsky SGS models in their original formulation as well as in their dynamic version.

First of all, the dynamic procedure has a remarkable effect on the amount of introduced SGS viscosity. In all the considered cases, the SGS viscosity produced in the wake by dynamic SGS models is significantly reduced compared to that given by their non-dynamic counterparts. An example is given in Figures 1 and 2, showing the instantantaneous iso-contours of μ_{sgs}/μ obtained in the VMS-LES simulations with the non-dynamic and dynamic WALE models respectively.

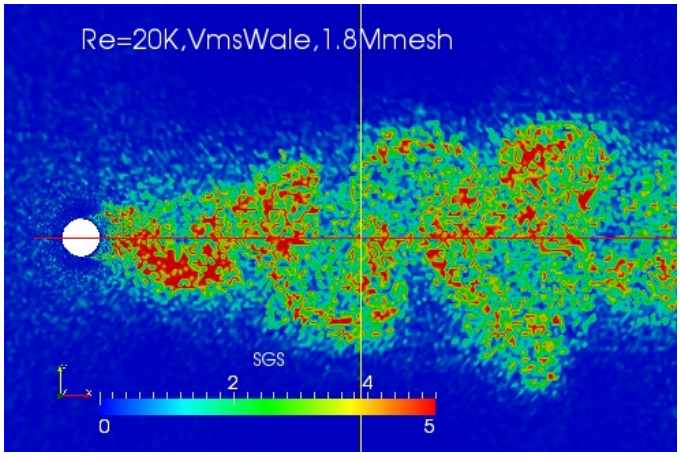

Fig. 1 Flow around a circular cylinder at Reynolds 20000 : viscosity ratio for the VMS-WALE.

The impact of these differences in SGS viscosity is investigated in terms of flow bulk parameters and statistics. For all simulations, statistics are computed by averaging in the spanwise homogeneous direction and in time for 30 vortex shedding cycles. The main bulk coefficients are summarized in Table 1. They are compared with the experimental results of [20] and [21] and with the data of the review in [22]. As for simulations we recall the LES results of [19], obtained with 2.3 million of cells, and of [18]. From this table, it appears that, except for the Smagorinsky SGS model within the LES approach, the bulk coefficients are in overall good agreement with the available numerical and experimental data. The maximum value of the turbulence intensity

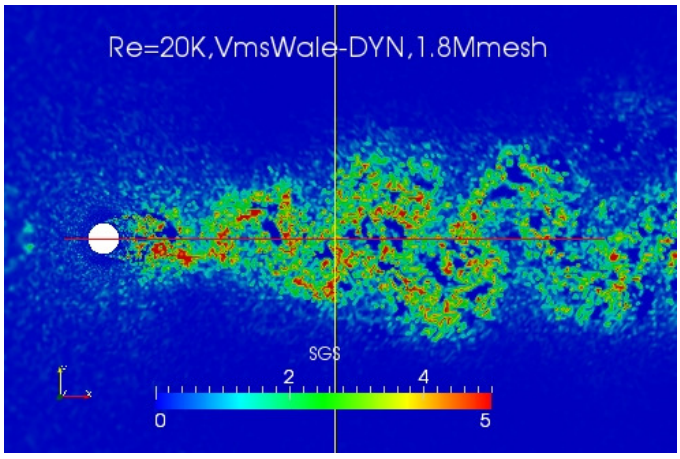

Fig. 2 Flow around a circular cylinder at Reynolds 20000 : viscosity ratio for the dynamic VMS-WALE.

	$\overline{C_d}$	C'_L	l_r	$\overline{-C_{pb}}$	St	Lv	I
LES Smagorinsky	**1.29**	**.59**	**.85**	**1.27**	**.19**	**.71**	**34.**
LES dyn. Smagorinsky	**1.21**	**.45**	**.93**	**1.20**	**.19**	**.96**	**34.5**
LES WALE	**1.16**	**.39**	**.97**	**1.15**	**.20**	**.71**	**31.5**
LES dyn. WALE	**1.19**	**.44**	**.92**	**1.16**	**.20**	**.96**	**31.8**
VMS Smagorinsky	**1.18**	**.43**	**.88**	**1.20**	**.20**	**.90**	**36.6**
VMS dyn. Smagorinsky	**1.19**	**.45**	**.95**	**1.19**	**.19**	**.96**	**31.8**
VMS WALE	**1.17**	**.42**	**.87**	**1.20**	**.20**	**.96**	**33.7**
VMS dyn. WALE	**1.18**	**.43**	**.89**	**1.19**	**.20**	**.96**	**32.8**
LES [18] **min.**	**.94**	**.17**	**.7**	**0.83**	–	–	–
max.	**1.28**	**.65**	**.4**	**1.38**	–	–	–
LES [19]	**1.20**	–	**.99**	**1.25**	–	**.99**	**38.1**
Exp. [20]	**1.16**	–	–	–	–	**1.0**	**37.0**
Exp. [21]	**1.20**	–	–	–	–	–	–
Exp. [22]	–	**.45**	–	**1.19**	**.19**	–	–

Table 1 Bulk flow parameters predicted by dynamic and non-dynamic VMS-LES around a circular cylinder at a Reynolds number of 20000. $\overline{C_d}$ holds for the mean drag coefficient, C'_L for the root mean square of lift, l_r is the recirculation length, $\overline{C_{pb}}$ is the mean pressure coefficient at cylinder basis, θ_{sep} is the separation angle, St is the Strouhal number, Lv denotes the x-location of the maximum in the turbulent intensity distribution, I holds for Max. turb. intensity.

for all the simulations carried out is underestimated compared to the experimental value. This is however not surprising, since as shown also in Figures 1 and 2, the contribution of the SGS model is significant in the very near wake region ($x/D < 2$), and it is not taken into account in the computation of the resolved turbulence intensity. From this table, it also appears that the impact of the dynamic procedure within the VMS-LES approach is rather small, and less important than with the LES approach. This can be explained by the fact that in the VMS-LES approach the SGS viscosity only acts on the smallest resolved scales, while this viscosity applies on all the resolved scales in classical LES. This observation is also confirmed by the mean pressure coefficient distribution at the cylinder, as shown in Figure 3 and 4.

A substantial improvement in the prediction of the distribution of the turbulence intensity can nevertheless be observed with the dynamic version of VMS-LES. This distribution along the wake centerline is depicted in Figures 5 and 6 for the non-dynamic and dynamic VMS-LES Smagorinsky respectively. These results are compared with those of Aradag [19] and the experimental data of Lim and Lee [20]. It can be seen that a good agreement with the experimental data is observed with the dynamic model both in the near wake and more downstream, while the Smagorinsky model does not only underestimate the intensiti of the peak, but it also gives a wrong prediction of its location.

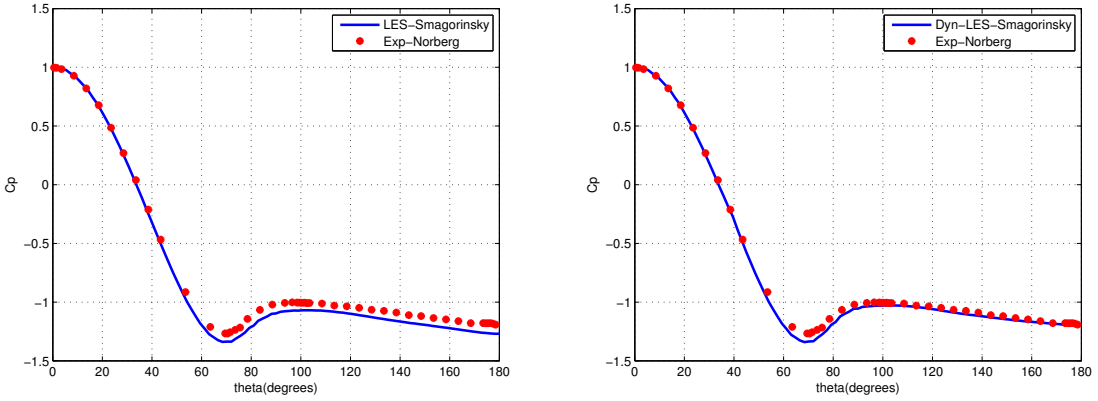

Fig. 3 Flow around a circular cylinder at Reynolds 20000 : mean pressure coefficient distribution at the cylinder from the LES Smagorinsky (left) and dyn. LES Smagorinsky (right) computation.

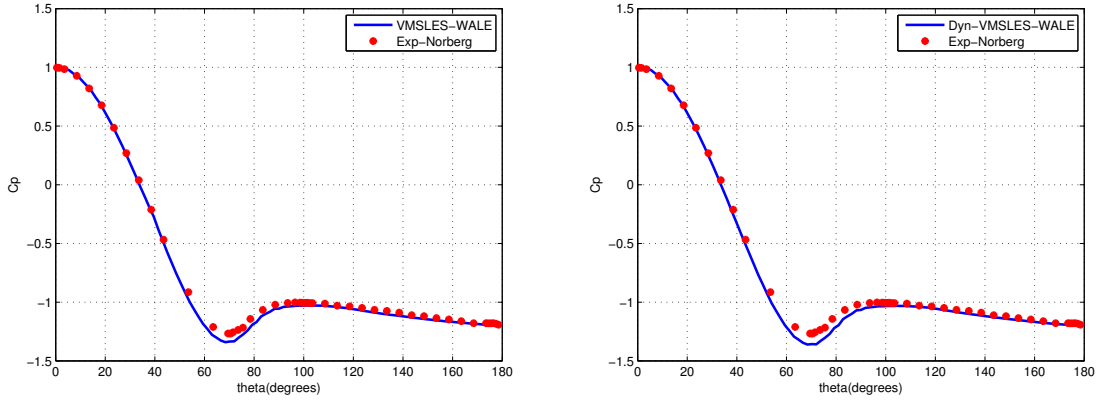

Fig. 4 Flow around a circular cylinder at Reynolds 20000 : mean pressure coefficient distribution at the cylinder from the VMS-LES WALE (left) and dyn. VMS-LES WALE (right) computation.

4.2 Cylinder test-case, Reynolds number 3900

In order to confirm that the dynamic procedure has an impact globally rather moderate within the VMS-LES approach, we consider now the flow around a circular cylinder at Reynolds number 3900. The computational domain is the same one used for the test-case Reynolds number 20000. The same boundary and freestream conditions, and the same numerical options, are used as for the previous case. The flow domain is discretized by two unstructured tetrahedral grids. The first one (GR1) contains approximately 290000 nodes, and the averaged distance of the nearest point to the cylinder boundary is 0.017D. The second grid (GR2) is obtained from GR1 by refining in a structured way, i.e. by dividing each tetrahedron in 8, resulting in approximately 1.46 million of nodes.

The same averaging procedure as for Reynolds 20000 is used in order to compute the statistics. The main bulk coefficients are summarized in Table 2.

The mean drag coefficient and the Strouhal number are in all cases in good agreement with the reference experimental data. For these bulk parameters the impact of dynamic SGS modeling seems to be almost negligible in the VMS-LES simulations, while it is significant but rather small for classical LES. As also pointed out in [24], the length of the mean recirculation bubble is noticeably underestimated on the coarser grid GR1, while the absolute value of the base pressure is overestimated. The use of dynamic SGS models on grid GR1 gives a small improvement in the prediction of these quantities, but good agreement with experimental data could be obtained only on the refined grid Gr2, independently of the SGS model.

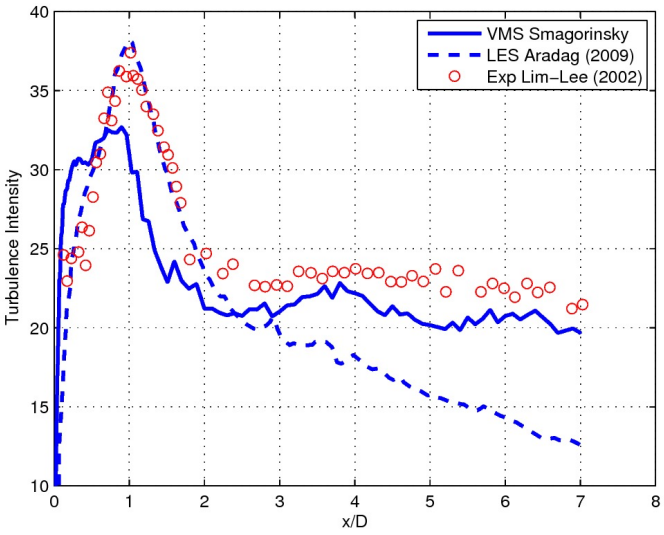

Fig. 5 Flow around a circular cylinder at Reynolds 20000 : distribution of the turbulence intensity along the wake centerline from the VMS-LES Smagorinsky computation.

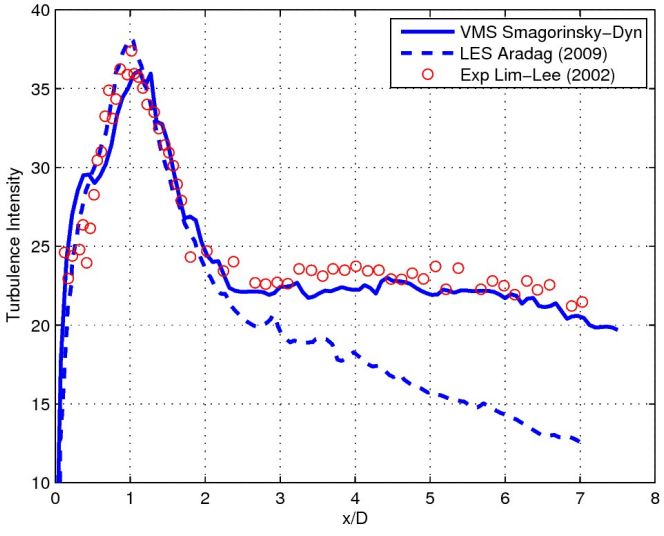

Fig. 6 Flow around a circular cylinder at Reynolds 20000 : distribution of the turbulence intensity along the wake centerline from the dynamic VMS-LES Smagorinsky computation.

The mean streamwise velocity profile along the wake centerline is reported in Figures 7 and 8 for VMS-LES WALE and its dynamic counterpart on the coarse grid (GR1) and the fine grid (GR2) respectively. These profiles confirm the observations previously made for the mean recirculation length. Indeed, it can be noted a rather poor prediction obtained on the coarser grid GR1, which is perfectly corrected by the use of the fine grid, and a slight improvement for both grids when the dynamic SGS model is active. This trend is confirmed by the prediction of the mean streamwise velocity profile at different streamwise locations depicted in Figures 9 and 10 for the coarse grid and the fine grid respectively. Once again the computation on grid GR2 is much more accurate with a rather significant improvement provided by the dynamic VMS method for both grids.

	$\overline{C_d}$	l_r	$-\overline{Cp_b}$	St
LES Smagorinsky (GR1)	**1.05**	**1.00**	**1.05**	**0.21**
LES dyn. Smagorinsky (GR1)	**0.99**	**1.13**	**1.07**	**0.219**
LES WALE (GR1)	**0.98**	**1.09**	**1.04**	**0.22**
LES dyn. WALE (GR1)	**0.94**	**1.13**	**0.99**	**0.22**
VMS Smagorinsky (GR1)	**1.03**	**1.00**	**1.11**	**0.217**
VMS dyn. Smagorinsky (GR1)	**1.01**	**1.05**	**1.08**	**0.219**
VMS WALE (GR1)	**1.00**	**0.96**	**1.10**	**0.22**
VMS dyn. WALE (GR1)	**0.97**	**1.10**	**1.04**	**0.22**
VMS WALE (GR2)	**0.94**	**1.47**	**0.81**	**0.22**
VMS dyn. WALE (GR2)	**0.94**	**1.47**	**0.85**	**0.22**
Exp. [23], min.	–	–	–	**0.205**
max.	–	–	–	**0.215**
Exp. [24], min.	–	**1.13**	–	–
max.	–	**1.23**	–	–
Exp. [25], min.	–	**1.41**	–	**0.206**
max.	–	**1.51**	–	**0.21**
Exp. Norberg (from [26]), min.	**0.94**	–	**0.83**	–
max.	**1.04**	–	**0.93**	–

Table 2 Bulk flow parameters predicted by dynamic and non-dynamic VMS-LES around a circular cylinder at a Reynolds number of 3900. Same symbols as previous tables.

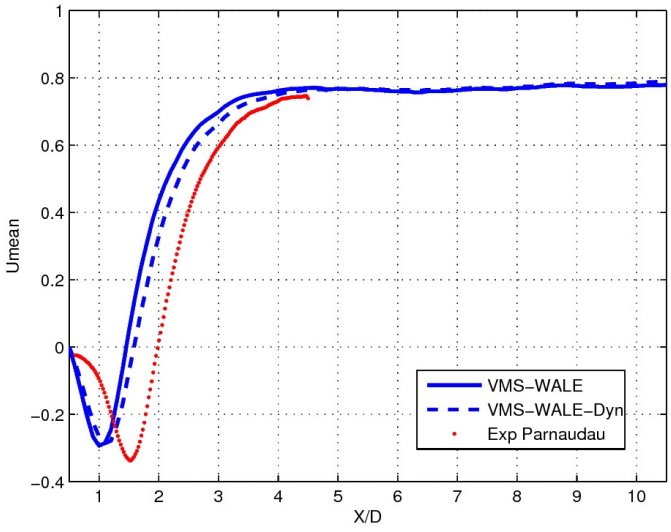

Fig. 7 Flow around a circular cylinder at Reynolds 3900 : mean streamwise velocity profile along the wake centerline for VMS-LES WALE and its dynamic counterpart on the coarse grid (GR1).

4.3 Square cylinder test-case, Reynolds number 22000

Obstacles with square or rectangular sections are extremely frequent in civil engineering structures, like buildings and bridges. The behavior of a flow past such an obstacle is quite different from the one around a circular cylinder. We restrict here to the case of a zero angle of attack.

Even for this case, the simulation is not trivial, although the separation is fixed by geometry and therefore the flow keeps similar properties for a large interval of Reynolds numbers, from 10000 to 200000. This type of flow is the object of a well-known benchmark [27] for a Reynolds number of 22000. This section focuses on this case. The overview in [27] points out that, in spite of the fixed separation, this flow is challenging for simulations, the main difficulty being the fact that the inflow is basically laminar, and transition takes place in the separate free shear layers on the side of the cylinder.

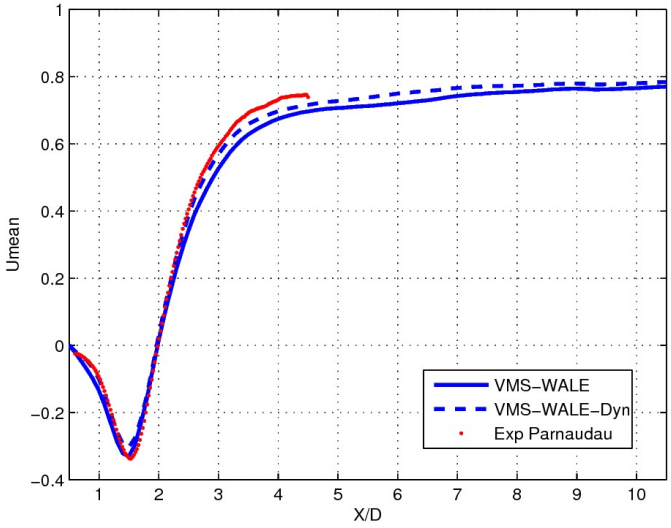

Fig. 8 Flow around a circular cylinder at Reynolds 3900 : mean streamwise velocity profile along the wake centerline for VMS-LES WALE and its dynamic counterpart on the fine grid (GR2).

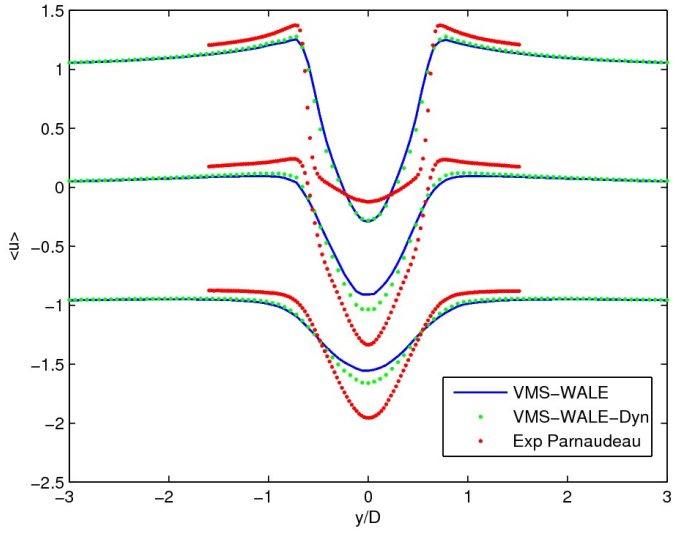

Fig. 9 Flow around a circular cylinder at Reynolds 3900 : mean streamwise velocity profile at $x/D = 1.06$ (top), $x/D = 1.54$ (center) and $x/D = 2.02$ (bottom), obtained for VMS-LES WALE and its dynamic counterpart on the coarse grid (GR1).

The mesh is radial such that its radius $R = 15D$, it involves 1210000 cells. As for the circular cylinder, periodic boundary conditions are applied in the spanwise direction and no-slip conditions are applied on the obstacle. Characteristic based conditions are used at the inflow and outflow. The freestream Mach number is also set equal to 0.1 Mean properties have been derived from a time interval containing 30 vortex-shedding cycles, using about 20000 time steps.

In Table 3 we compare a few bulk quantities for our non-dynamic and dynamic calculations with a DNS calculation by Verstappen *et al.*, (from the 1997 paper [28] and from more recent slides [29]) and measurements by Lyn *et al.*, [30,31], Luo *et al.*, [32].

The data of [30,31] and those of the simulations in [28] are in good accordance and can be used as a reference. As for the drag fluctuations, the values of [28] and [32] are in good agreement, but more recently in [29] a higher value is obtained closer to the outputs of our simulations. Conversely, the predictions of

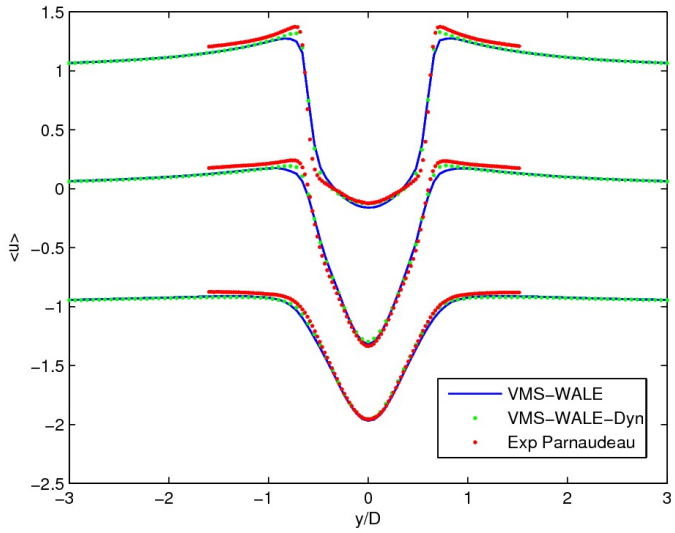

Fig. 10 Flow around a circular cylinder at Reynolds 3900 : mean streamwise velocity profile at $x/D = 1.06$ (top), $x/D = 1.54$ (center) and $x/D = 2.02$ (bottom), obtained for VMS-LES WALE and its dynamic counterpart on the fine grid (GR2).

	$\overline{C_d}$	l_r	St	C'_l	C'_d
VMS Smagorinsky	**2.08**	**0.74**	**0.127**	**1.38**	**0.25**
VMS dyn. Smagorinsky	**2.06**	**0.82**	**0.128**	**1.28**	**0.24**
DNS [28]	**2.09**	–	**0.133**	**1.45**	**0.178**
[29]	**2.1**	–	**0.133**	**1.22**	**0.21**
Exp. [30,31]	**2.1**	**0.88**	**0.133**	–	–
Exp. [32], Rey=34 000	**2.21**	–	**0.13**	**1.21**	**0.18**

Table 3 Bulk flow parameters predicted by dynamic and non-dynamic VMS-LES around a square cylinder at a Reynolds number of 22000. Same symbols as previous tables.

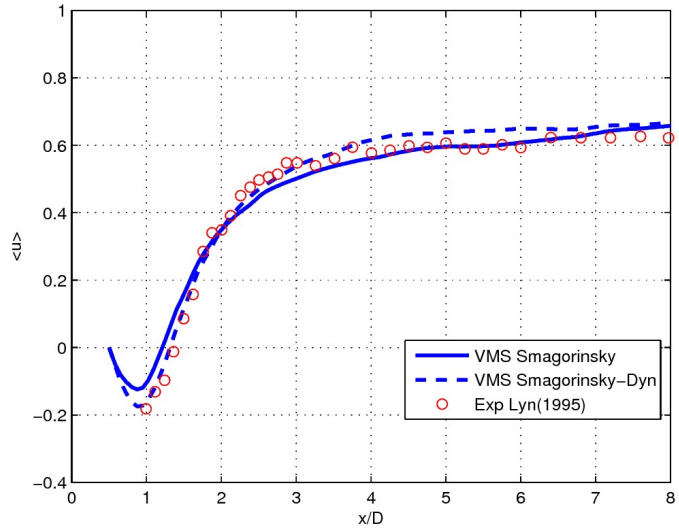

Fig. 11 Flow around a square cylinder at Reynolds 22000 : mean horizontal velocity on the centerline of the wake.

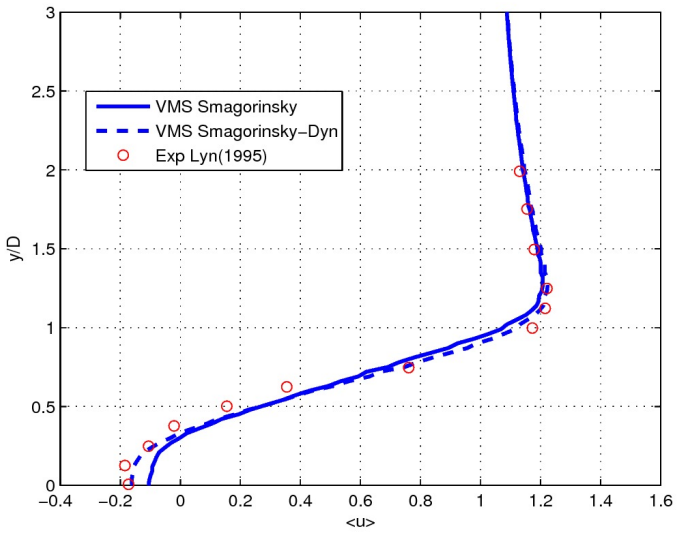

Fig. 12 Flow around a square cylinder at Reynolds 22000 : mean horizontal velocity at x/D=1.

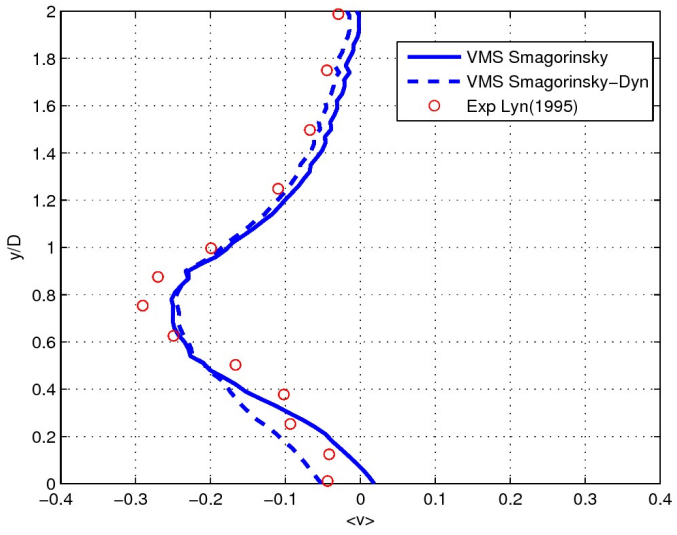

Fig. 13 Flow around a square cylinder at Reynolds 22000 : mean vertical velocity at x/D=1.

the fluctuating lift of [32] and [29] are in good agreement, while a larger value is given in [28]. Comparing with these experimental and DNS reference data, the accuracy of our computed bulk quantities seems to be noticeably improved by the combination of VMS and dynamic SGS models, except for the mean drag, whose prediction is however fairly good in both cases. Indeed $\overline{C_d}$ obtained with the standard Smagorinsky model is underestimated of less than 1% compared with the lowest boundary of the reference data range, while the underestimation increases to 1.4% with the dynamic model. On the other hand, the most significant improvement obtained with the dynamic SGS model is found in the prediction of the mean recirculation length. Indeed, l_r is underestimated of 16% by the standard Smagorinsky model and of 7% with its dynamic version.

Figures 11-14 show different mean velocity profiles obtained in our VMS-LES simulations with dynamic and non-dynamic Smagorinsky model, compared against the experimental data of [30,31]. In particular, Figures 11 and 12 show the profile of the mean streamwise velocity along the centerline of the wake and along the vertical axis at $x/D = 1$, while the profiles of the mean vertical velocity are reported in Figures 13 and 14 at

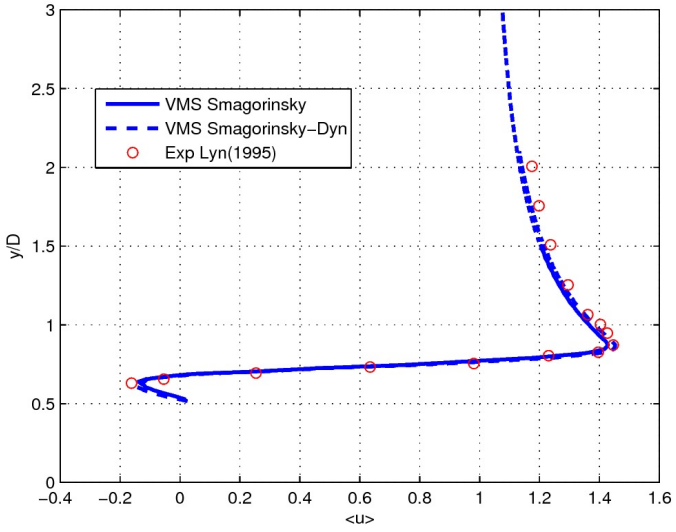

Fig. 14 Flow around a square cylinder at Reynolds 22000 : mean vertical velocity at x/D=0.

$x/D = 1$ and $x/D = 0$ respectively. The dynamic SGS models generally leads to a better agreement with the experimental data, although the differences with the results obtained by the classical Smagorinsky model are rather small.

4.4 Square cylinder test-case, Reynolds number 175000

As already mentioned, the higher Reynolds in this case is not expected to produce a very different flow, but to be more difficult to compute. Typically, mean pressure distribution and then mean drag are not supposed to change much, see Table 4. We find a recirculation zone notably shorter than for the smaller Reynolds number case, as it could have been expected, see Table 4 and compare it with Table 3, but we did not find any reference experimental result for this quantity. As for the other bulk parameters, the overall agreement with the reference data is good, with an underetimastion of 1.4% of the mean drag coefficient independently of the SGS model and an overestimation of the vortex shedding Strouhal number going from 5.7% for the standard Smagorinky model to 4% for its dynamic version. Once again the impact of dynamic SGS modeling is small, with slight improvements in the predictions of St and C'_d.

In Figure 15, which depicts the instantaneous vorticity magnitude field obtained in our calculations, one can notice that the dynamic VMS-LES computation, which introduces less SGS viscosity than the non-dynamic counterpart, is characterized by a larger number of small vortical structures, especially in the shear layers detaching from the cylinder corners.

	$\overline{C_d}$	l_r	St	C'_l	C'_d	$-\overline{C}_{pb}$
VMS Smagorinsky	**2.03**	**0.73**	**0.129**	**1.29**	**0.26**	**1.30**
VMS dyn. Smagorinsky	**2.03**	**0.75**	**0.127**	**1.26**	**0.23**	**1.30**
Exp. [33]	**2.06**	–	**0.122**	**1.21**	**0.23**	**1.30**
Exp. [34]	–	–	**0.12**	**1.32**	–	–

Table 4 Bulk flow parameters predicted by dynamic and non-dynamic VMS-LES around a square cylinder at a Reynolds number of 175000. Same symbols as in previous tables.

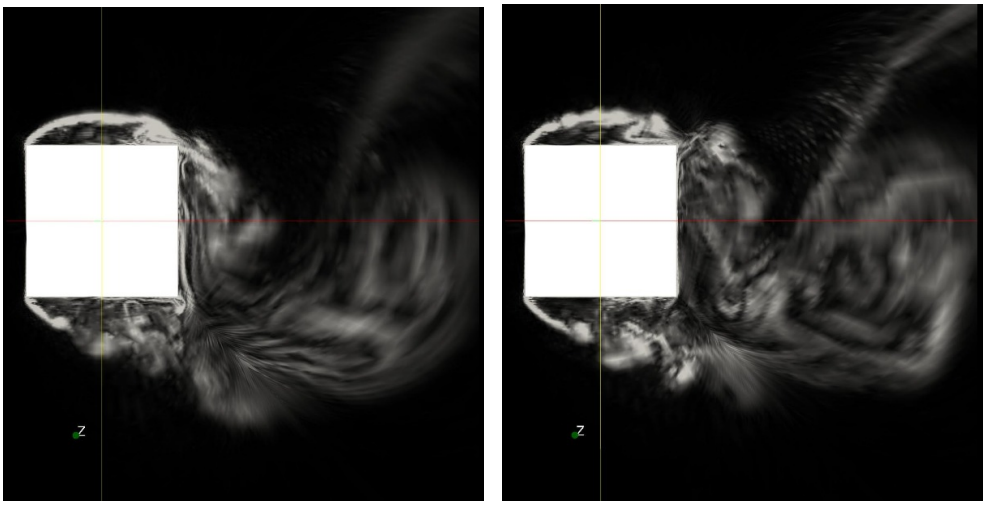

Fig. 15 Flow around a square cylinder at Reynolds 175000 : instantaneous vorticity field for the VMS-LES with the Smagorinsky model (left) and with its dynamic counterpart (right).

5 Conclusions

A variational multiscale LES approach combined with dynamic SGS models has been presented and appraised in the simulation of bluff-body flows in subcritical regimes. While the VMS approach selects which scales are damped by the SGS viscosity, the dynamic procedure selects in which regions a high damping is applied at different time instants. Somewhat surprisingly, previous works combining both tended to prove that the two methods give similar effects and cannot bring complementary improvements. In this paper we propose a non CPU-costly dynamic version and we re-examine this question by focusing on bluff-body flows. More specifically, the flow around a circular cylinder at Reynolds numbers 3900 and 20000 and the flow around a square cylinder at Reynolds 22000 and 175000 have been considered as benchmark tests.

The key ingredients of the numerics and modeling used in this work are the following: unstructured grids, a second-order accurate numerical scheme stabilized by a tunable numerical diffusion proportional to sixth-order space derivatives, and the VMS formulation combined with the dynamic and non-dynamic Smagorinsky and WALE SGS models. A set of rather coarse unstructured grids, as those often used in industrial applications, have been selected in order to get significant deviations between models, while obtaining rather good predictions.

We compared the bulk coefficients and the main flow features with experimental data and other numerical results in the literature.

We observed that the dynamic procedure importantly reduces the amount of introduced SGS viscosity with respect to that given by non-dynamic SGS models, both in classical and VMS LES simulations. However, it was found that, when combined with the VMS-LES approach, the effect of the dynamic procedure on bulk coefficients and main flow features has a smaller impact on the results than when used with a pure LES, which partly confirms the conclusions of previous works. This may be explained by the fact that the SGS viscosity only acts on the smallest resolved scales in the VMS-LES approach, while this viscosity applies to all the resolved scales in classical LES models.

Nevertheless, an overall improvement is observed with the combination of dynamic SGS modeling with the VMS approach. In particular, a notable improvement in the distribution of the turbulence intensity is obtained for the circular cylinder at Reynolds number 20000. and for the mean streamwise velocity profiles in the case of the circular cylinder at Reynolds number 3900. For the square cylinder at Reynolds number 22000, the examination of mean velocity profiles shows that deviations with respect to measurements in the recirculation zone produced by the non-dynamic Smagorinky VMS-LES model are in large part corrected by its dynamic version.

Since with a careful implementation the additional costs brougth by the dynamic procedure are very small, dynamic models may be considered an interesting option also within the VMS-LES approach.

Acknowledgements This work has been supported by French National Research Agency (ANR) through COSINUS program (project ECINADS n^o ANR-09-COSI-003). HPC resources from GENCI-[CINES] (Grant 2010-x2010026386 and 2010-c2009025067) are also gratefully acknowledged.

References

1. J. Smagorinsky, General circulation experiments with the primitive equations. *Monthl. Weath. Rev.*, 91(3) :99-164, 1963.
2. F. Nicoud and F. Ducros. Subgrid-scale stress modelling based on the square of the velocity gradient tensor. *Flow Turb. Comb.*, 62(3):183-200, 1999.
3. T.J.R. Hughes, L.Mazzei, and K.E. Jansen. Large-eddy simulation and the variational multiscale method. *Comput. Vis. Sci.*, 3:47-59, 2000.
4. B. Koobus and C. Farhat. A variational multiscale method for the large eddy simulation of compressible turbulent flows on unstructured meshes-application to vortex shedding. *Comput. Methods Appl. Mech. Eng.*, 193:1367-1383, 2004.
5. M. Germano, U. Piomelli, P. Moin, W.H. Cabot. A Dynamic Subgrid-Scale Eddy Viscosity Model. *Physics of Fluids*, A 3, 1760-1765, 1991.
6. D. K. Lilly. A proposed modification of the Germano subgrid scale closure model. *Physics of Fluids A*, 4:633-635, 1992.
7. C. Farhat, A. Rajasekharan, B. Koobus. A dynamic variational multiscale method for large eddy simulations on unstructured meshes. *Comput. Methods Appl. Mech. Engrg.*, 195 (2006) 1667-1691.
8. V. Gravemeier. Variational Multiscale Large Eddy Simulation of turbulent Flow in a Diffuser. *Computational Mechanics*, 39(4):477:495, 2012.
9. H. Ouvrard, B. Koobus, A. Dervieux, and M.V. Salvetti. Classical and variational multiscale LES of the flow around a circular cylinder on unstructured grids. *Computer and Fluids*, 39(7):1083âŁ"-1094, 2010.
10. S. Wornom, H. Ouvrard, M.-V. Salvetti, B. Koobus, A. Dervieux. Variational multiscale large-eddy simulations of the flow past a circular cylinder : Reynolds number effects. *Computer and Fluids*, 47(1):44âŁ"-50, 2011.
11. M.H. Lallemand, H. Steve, and A. Dervieux. Unstructured multigridding by volume agglomeration : current status. *Comput. Fluids*, 21:397-433, 1992.
12. H. Baya Toda, K. Truffin and F. Nicoud. Is the dynamic procedure appropriate for all SGS model. *V European Conference on Computational Fluid Dynamics*, ECCOMAS CFD, J.C.F. Pereira and A. Sequeira (Eds), Lisbon, Portugal, 14-17 June 2010.
13. S. Camarri, M.V. Salvetti, B. Koobus, and A. Dervieux. A low diffusion MUSCL scheme for LES on unstructured grids. *Comp. Fluids*, 33:1101-1129, 2004.
14. C. Farhat, B. Koobus and H. Tran. Simulation of vortex shedding dominated flows past rigid and flexible structures.*Computational Methods for Fluid-Structure Interaction*, 1-30, 1999.
15. P. L. Roe. Approximate Riemann solvers, parameters, vectors and difference schemes. *J. Comp. Phys*, 43:357-371, 1981.
16. B. Van. Leer. Towards the ultimate conservative scheme. IV :A new approach to numerical convection. *J. Comp. Phys.*, 23:276-299, 1977.
17. R. Martin and H. Guillard. A second-order defect correction scheme for unsteady problems. *Comput. and Fluids*, 25(1):9-27, 1996.
18. E. Salvatici and M.V. Salvetti, Large-eddy simulations of the flow around a circular cylinder: effects of grid resolution and subgrid scale modeling, *Wind & Structures*, 6(6):419-436, 2003.
19. S. Aradag. Unsteady turbulent vortex structure downstream of a three dimensional cylinder, *J. of Thermal Science and Technology*, 29(1):91-98, 2009.
20. H. Lim and S. Lee. Flow Control of Circular Cylinders with Longitudinal Grooved Surfaces, *AIAA Journal*, 40(10):2027-2035, 2002.
21. J.D. Anderson. *Fundamentals of Aerodynamics*, Second Edition, McGraw-Hill, New York, 1991.
22. C. Norberg. Fluctuating lift on a circular cylinder: review and new measurements. *J. Fluids Struct.*, 17:57-96, 2003.
23. L. Ong and J. Wallace. The velocity field of the turbulent very near wake of a circular cylinder. *Exp. Fluids*, 20:441âŁ"453, 1996.
24. L.M. Lourenco and C. Shih. Characteristics of the plane turbulent near wake of a circular cylinder. a particle image velocimetry study, (data taken from Kravchenko and Moin).
25. P. Parnaudeau, J. Carlier, D.Heitz and E. Lamballais. Experimental and numerical studies of the flow over a circular cylinder at Reynolds number 3900. *Phys. Fluids*, 20(085101), 2008.
26. A.G. Kravchenko and P. Moin. Numerical studies of flow over a circular cylinder at re=3900. *Phys. Fluids*, 12(2):403âŁ"417, 1999.
27. W. Rodi, J.H. Ferziger, M. Breuer and M. Pourqui "Status of Large Eddy Simulation: Results of a Workshop" *J. Fluids Engineering*, Transactions of the ASME, 119, 248-262, (1997).
28. R.W.C.P. Verstappen and A.E.P. Veldman, Direct numerical simulation of turbulence at lower costs. *Journal of Engineering Mathematics*, 32:143âŁ"159, 1997.
29. R. Verstappen. Regularizing turbulent flow, 2010. *http://www.prace-ri.eu/IMG/pdf/16-verstappen.pdf*
30. D. A. Lyn and W. Rodi The flapping shear layer formed by flow separation from the forward corner of a square cylinder *J. Fluid Mech.* 261:353-316, 1994.
31. D. A. Lyn, S. Einav, W. Rodi and J-H. Park, A laser-Doppler velocimetry study of ensemble-averaged characteristics of the turbulent near wake of a square cylinder. *J . Fluid Mech.* 304:285-319, 1995.
32. S. C. Luo and MdG. Yazdani and Y. T. Chew and T. S. Lee, Effects of incidence and afterbody shape on flow past bluff cylinders, *J. Ind. Aerodyn.*, 53:375-399, 1994.
33. B.E. Lee, The effect of turbulence on the surface pressure field of a square prism. *J. Fluid Mech.*, 69:263-282, 1975.
34. B.J. Vickery. Fluctuating lift and drag on a long cylinder of square cross-section in a smooth and in a turbulent stream. *Fluid Mech*, 25:481-494, 1966.